Biophysical Journal, Volume *115*

Supplemental Information

Phragmoplast Orienting Kinesin 2 Is a Weak Motor Switching between Processive and Diffusive Modes

Mayank Chugh, Maja Reißner, Michael Bugiel, Elisabeth Lipka, Arvid Herrmann, Basudev Roy, Sabine Müller, and Erik Schäffer

Biophysical *Journal*
Supporting Material

Phragmoplast Orienting Kinesin 2 is a weak motor switching between processive and diffusive modes

Mayank Chugh[1], Maja Reißner[1], Michael Bugiel[1], Elisabeth Lipka[2], Arvid Herrmann[2], Basudev Roy[1,3], Sabine Müller[2], and Erik Schäffer[1,*]

[1]Cellular Nanoscience, Center for Plant Molecular Biology (ZMBP), University of Tübingen, Auf der Morgenstelle 32, 72076 Tübingen, Germany
[2]Developmental Genetics, Center for Plant Molecular Biology (ZMBP), University of Tübingen, Auf der Morgenstelle 32, 72076 Tübingen, Germany
[3]Current address: Department of Physics, Indian Institute of Technology, Madras 600036, India
[*]Correspondence: erik.schaeffer@uni-tuebingen.de

CONTENTS

LIST OF FIGURES

S1 SUPPLEMENTARY VIDEOS

VIDEO S1 Motility of single $POK2_{1-589}$ on microtubules. Image sequence of single $POK2_{1-589}$ (green) interacting with a microtubule (red) corresponding to the third panel of Fig. 1c. Still images are displayed in Fig. 1e. The video is 11 μm wide and 17× real time.

S2 SUPPLEMENTARY FIGURES

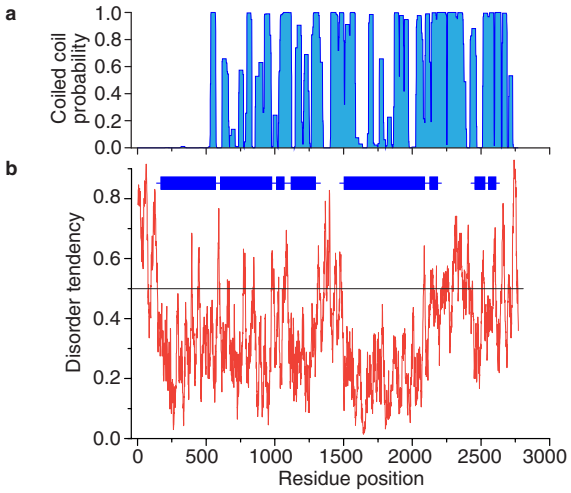

FIGURE S1 Protein domains of full-length POK2. **(a)** The coiled-coils prediction plot based on PCOILS (toolkit.tuebingen.mpg.de/#/tools/pcoils). Window size was 28. The predictions are consistent with MARCOILS (toolkit.tuebingen.mpg.de/#/tools/marcoil). **(b)** Disorder prediction plot based on IUPRED (iupred.enzim.hu). The blue bars indicate predicted globular/structured regions, while the red line represents disorder tendency estimated from pairwise amino acid energy content. The black line indicates the threshold.

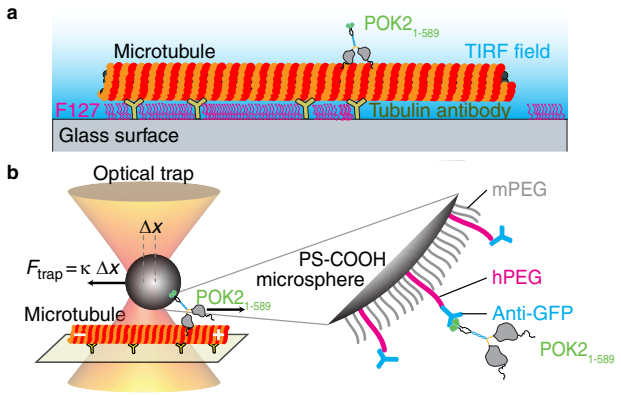

FIGURE S2 Schematic representation of *in vitro* assays. **(a)** Experimental setup for motility assays conducted using TIRF microscopy. $POK2_{1-589}$ specifically interacts with a microtubule bound via antibodies to a hydrophobic glass surface. **(b)** Illustration on an optical tweezers, $POK2_{1-589}$-microsphere coupling, and force measurement assays. In the presence of ATP, $POK2_{1-589}$ motors pull the microspheres out of the optical trap. The force is proportional to the displacement $F = \kappa\Delta x$, where κ is the trap stiffness and Δx the microsphere displacement from the stationary trap center. Pluoronic F127 is used in both assays to prevent unspecific interactions. GFP antibodies are covalently coupled via heterofunctional polyethylene glycol (hPEG), to carboxylated polystyrene microspheres (PS-COOH). Monofunctional PEG (mPEG) molecules prevent unspecific interactions.

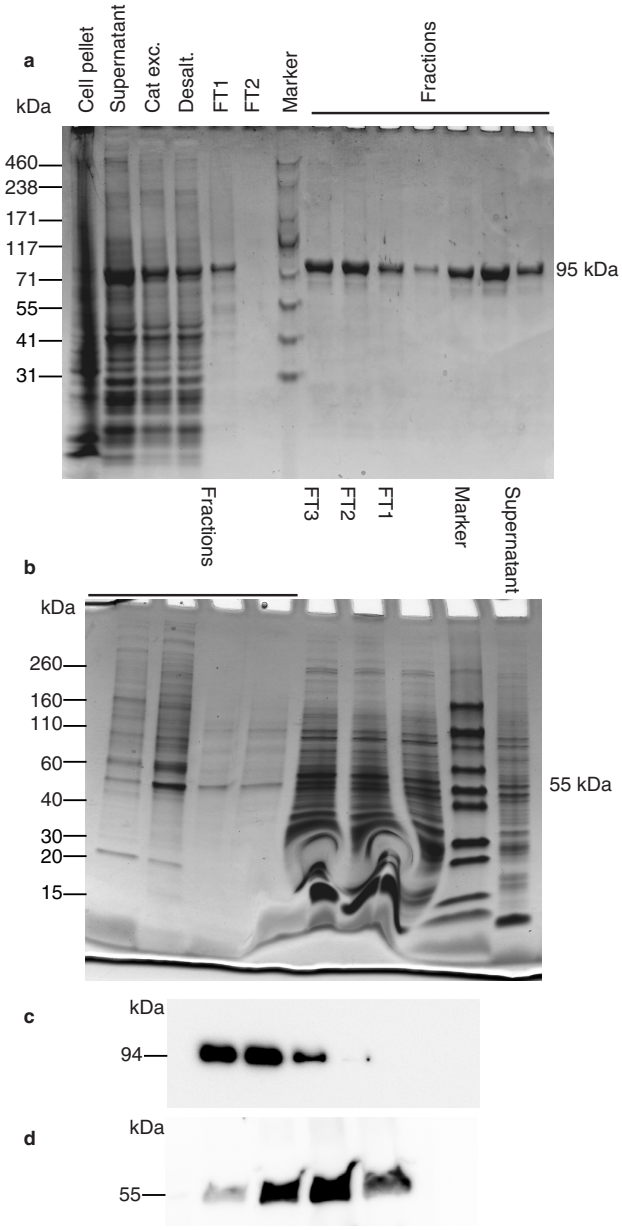

FIGURE S3 Quality control of $POK2_{1-589}$ and $POK2_{183-589}$ post-purification. **(a-b)** Coomassie-stained 4–20% Tris-Glycine SDS-PAGE gel showing purified protein fractions (95 kDa and 55 kDa) for $POK2_{1-589}$ and $POK2_{183-589}$ in **(a)** and **(b)**, respectively. Fractions denote collected protein eluates. (Cat exc.: cation exchange eluate, Desalt.: desalting eluate, FT: flow through). **(c-d)** Western blots against anti-GFP for the eluted proteins fractions of $POK2_{1-589}$ and $POK2_{183-589}$ in **(c)** and **(d)**, respectively.

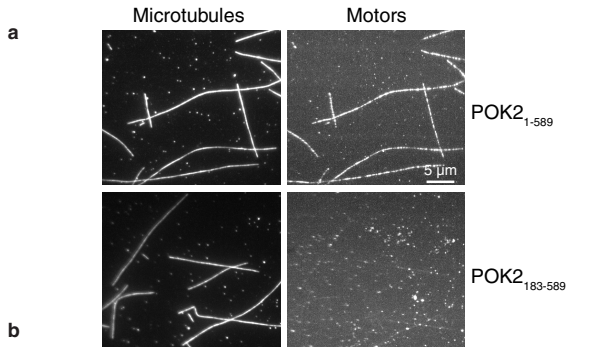

FIGURE S4 Reduced affinity of the POK2$_{183-589}$ towards the microtubule lattice. **(a)** Maximum projections representing the co-localization of motors onto the microtubule lattice in 1mM AMP-PNP. Images were acquired using TIRF microscopy under the same conditions and contrast. Even though the POK2$_{183-589}$ concentration was about twice that of POK2$_{1-589}$ based on the western blot and NanoDrop quantification, much less POK2$_{183-589}$ bound to the microtubules during the same amount of time. **(b)** Multiple sequence alignment (MSA) of the POK2 N-terminal extension (Nte) with BimC. The MSA was performed using Clustal Omega with default parameters (https://toolkit.tuebingen.mpg.de/#/tools/clustalo). Asterisks signify conserved residues, colons represent conservation among amino acids exhibiting strongly similar properties, and periods mark conservation among amino acids exhibiting weakly similar properties. Positively charged residues that may interact with the negatively charged tubulin e-hooks are indicated in red.

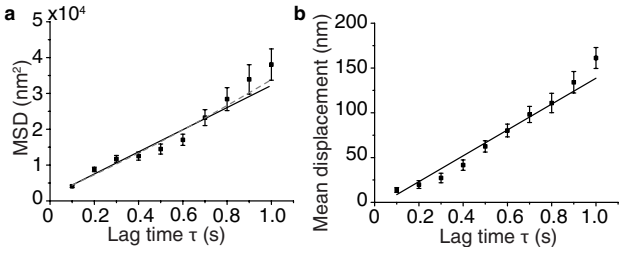

FIGURE S5 Diffusive segments exhibit bias. **(a)** Mean-squared displacement (MSD) and **(b)** mean displacement versus time lag τ for diffusive segments (mean ± SEM). A linear fit (black line) in **(a)** resulted in a diffusion coefficient of 0.015 ± 0.001 μm^2/s. A parabolic fit (grey dashed line) did not result in a significant speed. A linear fit (black line) in **(b)** resulted in a directed bias of 140 ± 10 nm/s. All fits were weighted by the error bars.

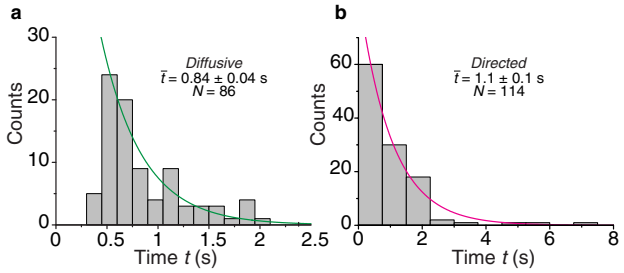

FIGURE S6 POK2$_{1-589}$–microtubule-interaction times of diffusive and directed segments. Time distributions for **(a)** diffusive and **(b)** directed segments (mean ± SEM and number of molecules are indicated, single exponentials are plotted as a guide to the eye).

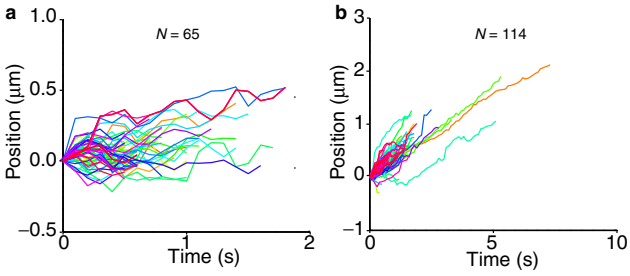

FIGURE S7 POK2$_{1-589}$ diffusive and directed segment trajectories. Trajectories of **(a)** all diffusive and **(b)** all directed segments from tracked single POK2$_{1-589}$ molecules. All segments are offset such that they start at zero.

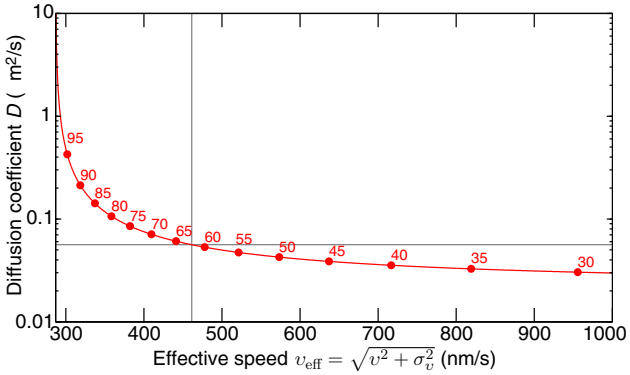

FIGURE S8 Relation between diffusion coefficient and effective speed. Dependence of the diffusion coefficient on the effective speed according to Eq. 12 (red line) for a set of fit parameters resulting from a parabolic fit to the MSD relation. Specific directed-mode time fractions ϕ (Eq. 13) are indicated by the red circles and numbers. Grey lines indicate the values for POK2$_{1-589}$.

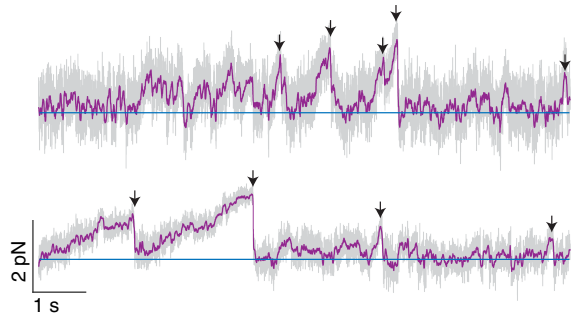

FIGURE S9 Multiple motors can exert higher force. Force traces of microspheres powered by multiple $POK2_{1-589}$ as a function of time. A 10× higher incubation concentration of $POK2_{1-589}$ with microspheres was used compared to the single-molecule assays resulting in the motility of 5 out of 6 microspheres. The blue line marks zero force. Arrow heads point to the maximum force prior to detachment events.

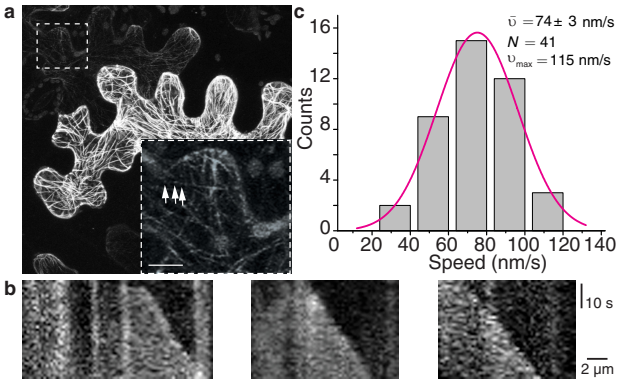

FIGURE S10 *In vivo* speeds of transiently expressed $POK2_{1-589}$ **(a)** Tobacco leaf epidermis show varying levels of 35S:GFP-$POK2_{1-589}$ expression. Cells with low and discontinuous GFP signal (boxed) were used for further *in vivo* analysis. Scale bar: 25 μm. Enlargement of the boxed region confirms low abundance of GFP-$POK2_{1-589}$. Scale bar: 8 μm. Arrow heads point towards the accumulations of GFP-$POK2_{1-589}$ along the linear trajectories. **(b)** Examples of kymographs. **(c)** Frequency distribution of *in vivo* speeds of GFP-$POK2_{1-589}$ (N = 41, combined from five cells from three different plants and two independent transformations).

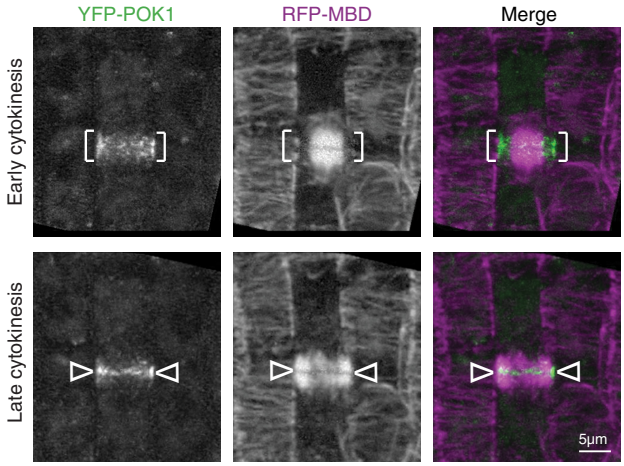

FIGURE S11 Narrowing of cortical division site. *Arabidopsis* root meristem expressing YFP-POK1 and RFP-MBD indicating narrowing of the division site from early cytokinesis to the presumably cell plate fusion site during late cytokinesis. For experimental details see reference (7) of the main text.